

Supporting Information

Engineering of NADPH Supply Boosts Photosynthesis-Driven Biotransformations

Leen Assil-Companioni^{a,b#}, Hanna C. Büchsenschütz^{a#}, Dániel Solymosi^c, Nina G. Dyczmons-Nowaczyk^d, Kristin K. F. Bauer^a, Silvia Wallner^e, Peter Macheroux^e, Yagut Allahverdiyeva^c, Marc M. Nowaczyk^{d*} and Robert Kourist^{a*}

^a Institute of Molecular Biotechnology, Graz University of Technology, Petersgasse 14, 8010 Graz, Austria.

^bACIB GmbH, Petergasse 14, 8010 Graz, Austria

^c Molecular Plant Biology unit, Department of Biochemistry, Faculty of Science and Engineering, University of Turku, Turku 20014, Finland

^d Department of Plant Biochemistry, Faculty of Biology & Biotechnology, Ruhr University Bochum, 44780 Bochum, Germany

^e Institute of Biochemistry, Graz University of Technology, Petersgasse 10, 8010 Graz, Austria

#authors contributed equally to this work

*corresponding authors: kourist@tugraz.at and marc.m.nowaczyk@rub.de

Table of Contents

List of Abbreviations	3
Supporting Tables	4
<i>Table S1</i>	4
<i>Table S2</i>	5
<i>Table S3</i>	6
<i>Table S4</i>	7
Supporting Figures	8
<i>Figure S1</i>	8
<i>Figure S2</i>	9
<i>Figure S3</i>	10
<i>Figure S4</i>	11
<i>Figure S5</i>	12
<i>Figures S6, S7, S8</i>	13
<i>Figure S9</i>	15
<i>Figures S10 and S11</i>	16
<i>Figure S12</i>	17
<i>Figure S13</i>	18
<i>Figure S14 and S15</i>	19
<i>Figure S16 and S17</i>	20
<i>Figure S18 and S19</i>	22
References	23

List of Abbreviations

In alphabetical order

1a	2-methylmaleimide
1b	2-methylsuccinimide
2a	<i>N</i> -methylmaleimide
2b	<i>N</i> -methylsuccinimide
3a	2-methyl- <i>N</i> -methylmaleimide
3b	2-methyl- <i>N</i> -methylsuccinimide
4a	cyclohexenone
4b	cyclohexanone
5a	2-methylcyclohexenone
5b	2-methylcyclohexanone
AL	Actinic light
BSA	Bovine serum albumin
chl_a	Chlorophyll <i>a</i>
cyt	Cytochrome
DCW	Dry cell weight
Fd	Ferredoxin
Flv	Flavodiiron protein
FNR	Fd-NADP ⁺ reductase
GC-FID	Gas chromatography- flame ionization detector
Mat&Met	Materials and methods
NDH-1	type I NADH dehydrogenase complex
OD₇₅₀	Optical density (measured at 750 nm)
OYE	Old yellow enzyme
PAM	Pulse amplitude modulation
PBS	Phosphate buffered saline
PET	Photosynthetic electron transport chain
PQ	Plastoquinone
PSI	Photosystem I
PSII	Photosystem II
S.I.	Supporting information
Synechocystis / Syn	<i>Synechocystis</i> sp. PCC 6803
WT	Wildtype
Y (I)	Effective yield of photosystem I
Y (II)	Effective yield of photosystem II

Supporting Tables

Table S1

Strains and plasmids

Table S1 List of strains and plasmid which appear in this work and were used for the construction of the recombinant strains

Strain/Plasmid	Description	Reference
SynRekB_P _{psbA2} YqjM	Integrative plasmid, P _{psbA2} promoter, His-tag (N), ene-reductase YqjM from <i>Bacillus subtilis</i>	1
SynRekB_P _{cpc} YqjM	Integrative plasmid, P _{cpc} promoter, His-tag (N), ene-reductase YqjM from <i>Bacillus subtilis</i>	This work
SynRekB_P _{zia} YqjM	Integrative plasmid, P _{zia} promoter, His-tag (N), ene-reductase YqjM from <i>Bacillus subtilis</i>	This work
<i>Escherichia coli</i> TOP 10 F'	F- <i>mcrA</i> Δ(<i>mrr-hsdRMS-mcrBC</i>) φ80/ <i>lacZ</i> ΔM15 Δ <i>lacX74 recA1 araD139 Δ(ara-leu)7697 gaU gaK</i> λ ⁻ rpsL(Str ^R) <i>endA1 nupG</i>	-
<i>Synechocystis</i> sp. PCC 6803 (Syn WT)	Cyanobacterium used for light-driven whole-cell biotransformations, geographical origin in California (USA)	2
<i>Synechocystis</i> sp. PCC 6803 ΔFlv1	<i>Synechocystis</i> sp. PCC 6803 knock-out strain lacking flavodiiron protein Flv1 <i>Provided by Prof. Yagut Allahverdiyeva-Rinne</i>	3
<i>Synechocystis</i> sp. PCC 6803 ΔFlv3	<i>Synechocystis</i> sp. PCC 6803 knock-out strain lacking flavodiiron protein Flv3 <i>Provided by Prof. Yagut Allahverdiyeva-Rinne</i>	3
<i>Synechocystis</i> sp. PCC 6803 P _{zia} YqjM (Syn::P _{zia} YqjM)	Transgenic <i>Synechocystis</i> sp. PCC 6803 strain constructed in WT background <i>via</i> homologous recombination using SynRekB_P _{zia} YqjM. The strain harbours the gene of YqjM controlled by the P _{zia} promoter in the genome locus <i>slr0168</i>	This work
<i>Synechocystis</i> sp. PCC 6803 P _{psbA2} YqjM (Syn::P _{psbA2} YqjM)	Transgenic <i>Synechocystis</i> sp. PCC 6803 strain constructed in WT background <i>via</i> homologous recombination using SynRekB_P _{psbA2} YqjM. The strain harbours the gene of YqjM controlled by the P _{psbA2} promoter in the genome locus <i>slr0168</i>	1
<i>Synechocystis</i> sp. PCC 6803 P _{cpc} YqjM (Syn::P _{cpc} YqjM)	Transgenic <i>Synechocystis</i> sp. PCC 6803 strain constructed in WT background <i>via</i> homologous recombination using SynRekB_P _{cpc} YqjM. The strain harbours the gene of YqjM controlled by the P _{cpc} promoter in the genome locus <i>slr0168</i>	This work
<i>Synechocystis</i> sp. PCC 6803 ΔFlv1 P _{cpc} YqjM (ΔFlv1::P _{cpc} YqjM)	Transgenic <i>Synechocystis</i> sp. PCC 6803 strain constructed in ΔFlv1 background <i>via</i> homologous recombination using SynRekB_P _{cpc} YqjM. The strain harbours the gene of YqjM controlled by the P _{cpc} promoter in the genome locus <i>slr0168</i>	This work
<i>Synechocystis</i> sp. PCC 6803 ΔFlv3 P _{cpc} YqjM (ΔFlv3::P _{cpc} YqjM)	Transgenic <i>Synechocystis</i> sp. PCC 6803 strain constructed in ΔFlv3 background <i>via</i> homologous recombination using SynRekB_P _{cpc} YqjM. The strain harbours the gene of YqjM controlled by the P _{cpc} promoter in the genome locus <i>slr0168</i>	This work

Table S2

List of primers

Table S2 Primers used in this study. For primers with overhangs, underlined parts denote the sequences complementary to the template.

Primer	Function	Sequence
Kan_rv	sequencing	GGGCTTCCCATACAATCGATAG
Seq_promoter_fw	sequencing	CTATTCAATACACCCCCTAAGCTAG
Seq_psbA2_fw	sequencing	CTTTAGACTAAGTTTAGTCAGTTC
Seq_cpc_fw	sequencing	TAGGGTCATTACTTTGGAC
Seq_zia_fw	sequencing	GAGCTAGGGAAAAATTTAAACTGG
Seg_fw	segregation check	TGGCCCTGGACAGTCAGGAATG
Seg_rv	segregation check	GCTGCATGTTGGGACTGGAGAC
P21	linearization primer FC	ATGCATCACCATCACCATCAC
P11	linearization primer FC	GTCTAGCTTAGGGGGTGTATTGAATAGTC
P19	Insert amplification P _{zia}	GACTATTCAATACACCCCCTAAGCTAGACTCAT CGTCCATCTCCTTAATCCGATTC
P22	Insert amplification P _{zia}	GTGATGGTGATGGTGATGCATGGCGGCCAACG TGATTTAAAGAAAAAC
P13	Insert amplification P _{cpc}	GACTATTCAATACACCCCCTAAGCTAGACCCCA TTAGCAAGGCAAATC
P36	Insert amplification P _{cpc}	CGTGATGGTGATGGTGATGCATIGAATTAATCT CCTACTTGACTTTATG

Table S3

Light intensity measurements

This table shows the intensity of photosynthetically active radiation (PAR) measured for 'high light cultivation'. The measurements were done with a LI-90 PAR sensor affixed to the rotary shaker and a submersible quantum microsphere set at a depth of 1mm. Values were measured when the rotary shaker was off and on. The values presented here were measured at the beginning of the cultivation phase with cultures that had an optical density of 0.05-0.1. A graphical schematic of the set up and measurements can be found in Figures **S10** and **S11**.

Table S3 Table showing recorded PAR values (in $\mu\text{E m}^{-2} \text{s}^{-1}$) recorded on a LI-COR LI-250A meter. Measurements presented are derived from values averaged across 15 seconds of measurements. Knob setting refers to increments on the blue-red light panel used to provide illumination and was set equally for both the blue and red LEDs.

Knob Setting (on both LED panels)	LI-90R sensor (affixed to shaker surface)		Submersible Sensor (set at a depth of ~ 1mm)	
	Shaking ON	Shaking OFF	Shaking ON	Shaking OFF
2	147.68	146.59	100.35	96.84
3	190.85	190.76	132.75	103.59

Table S4

GC-FID method

Table S4 Parameters for the GC-FID methods that were used to detect the substrates and products 1-5.

		1a-b	2a-b, 3a-b	4a-b	5a-b																																							
Column parameter	Column	ZB-5, ID 342390			Hydroxy β -TBDAC																																							
	Film Thickness	0.25 μm			0.25 μm																																							
	Column length	30 m			50 m																																							
	Inner Diameter	0.32 mm			0.25 mm																																							
	Stat. phase	5 % Phenyl 95 % Dimethylpolysiloxane			heptakis-(2,3-di-O-acetyl-6-O-t-butyl-dimethylsilyl)- β -cyclodextrin																																							
Autosampler and Injection Port	Injection Volume	1 μL																																										
	Injection Temp.	230 $^{\circ}\text{C}$																																										
	Carrier Gas	N_2																																										
	Total Flow	19.8 mL min^{-1}	21.6 mL min^{-1}	24 mL min^{-1}	146.2 mL min^{-1}																																							
	Column Flow	0.80 mL min^{-1}	0.88 mL min^{-1}	1 mL min^{-1}	1.42 mL min^{-1}																																							
	Linear Velocity	17.6 cm s^{-1}	17.6 cm s^{-1}	19.6 cm s^{-1}	30 cm s^{-1}																																							
	Purge Flow	3 mL min^{-1}																																										
	Split Ratio	20																																										
Temperature program		<table border="1"> <thead> <tr> <th>Rate [$^{\circ}\text{C}/\text{min}$]</th> <th>Tem. [$^{\circ}\text{C}$]</th> <th>hold [min]</th> </tr> </thead> <tbody> <tr> <td>---</td> <td>100</td> <td>3</td> </tr> <tr> <td>30</td> <td>310</td> <td>4</td> </tr> </tbody> </table>	Rate [$^{\circ}\text{C}/\text{min}$]	Tem. [$^{\circ}\text{C}$]	hold [min]	---	100	3	30	310	4	<table border="1"> <thead> <tr> <th>Rate [$^{\circ}\text{C}/\text{min}$]</th> <th>Tem. [$^{\circ}\text{C}$]</th> <th>hold [min]</th> </tr> </thead> <tbody> <tr> <td>---</td> <td>60</td> <td>5</td> </tr> <tr> <td>30</td> <td>310</td> <td>4</td> </tr> </tbody> </table>	Rate [$^{\circ}\text{C}/\text{min}$]	Tem. [$^{\circ}\text{C}$]	hold [min]	---	60	5	30	310	4	<table border="1"> <thead> <tr> <th>Rate [$^{\circ}\text{C}/\text{min}$]</th> <th>Tem. [$^{\circ}\text{C}$]</th> <th>hold [min]</th> </tr> </thead> <tbody> <tr> <td>---</td> <td>60</td> <td>5</td> </tr> <tr> <td>10</td> <td>200</td> <td>3</td> </tr> <tr> <td>25</td> <td>300</td> <td>3</td> </tr> </tbody> </table>	Rate [$^{\circ}\text{C}/\text{min}$]	Tem. [$^{\circ}\text{C}$]	hold [min]	---	60	5	10	200	3	25	300	3	<table border="1"> <thead> <tr> <th>Rate [$^{\circ}\text{C}/\text{min}$]</th> <th>Tem. [$^{\circ}\text{C}$]</th> <th>hold [min]</th> </tr> </thead> <tbody> <tr> <td>---</td> <td>90</td> <td>3</td> </tr> <tr> <td>5</td> <td>220</td> <td>3</td> </tr> </tbody> </table>	Rate [$^{\circ}\text{C}/\text{min}$]	Tem. [$^{\circ}\text{C}$]	hold [min]	---	90	3	5	220	3
	Rate [$^{\circ}\text{C}/\text{min}$]	Tem. [$^{\circ}\text{C}$]	hold [min]																																									
---	100	3																																										
30	310	4																																										
Rate [$^{\circ}\text{C}/\text{min}$]	Tem. [$^{\circ}\text{C}$]	hold [min]																																										
---	60	5																																										
30	310	4																																										
Rate [$^{\circ}\text{C}/\text{min}$]	Tem. [$^{\circ}\text{C}$]	hold [min]																																										
---	60	5																																										
10	200	3																																										
25	300	3																																										
Rate [$^{\circ}\text{C}/\text{min}$]	Tem. [$^{\circ}\text{C}$]	hold [min]																																										
---	90	3																																										
5	220	3																																										
FID detector	Temperature	320 $^{\circ}\text{C}$																																										
	Sampling rate	40 ms																																										
	H_2 flow	40 mL min^{-1}																																										
	Air flow	400 mL min^{-1}																																										
Ret. time	Substrate	5.6 min	6.8 min / 7.3 min	8.7 min	14.4 min																																							
	Product	6.2 min	7.3 min / 8.5 min	7.8 min	12.2 min (R) / 12.3 min (S)																																							
	Decanol	7.2 min	9.6 min	15.0 min	18.7 min																																							

Supporting Figures

Figure S1

Qualitative SDS-PAGE

Samples were mixed with sample buffer and denatured (10 min, 95 °C) before being loaded onto a precast acrylamide gel (GenScript, ExpressPlus™ PAGE Gel, 10×8, 4-12 %, 12 wells). After gel electrophoresis using Tris-MOPS-SDS running buffer (ThermoFisher Scientific, catalog number: M00138), gels were stained with Coomassie Brilliant Blue.

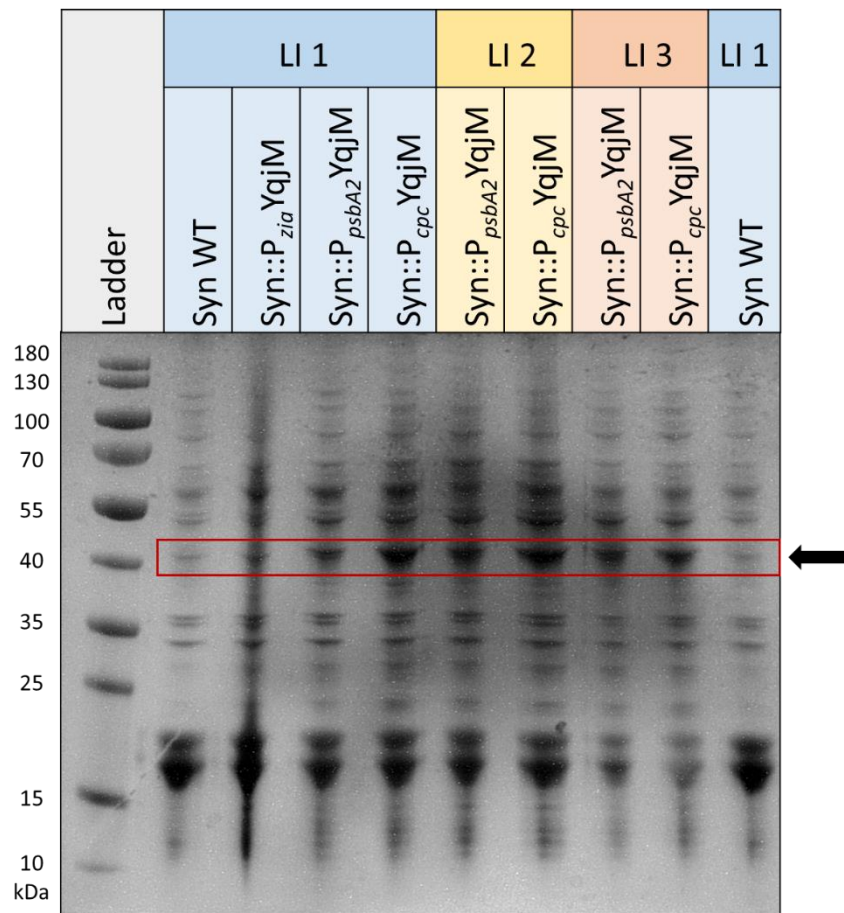


Figure S1 Figure depicts an SDS PAGE gel with crude cell extracts from different strains grown under differing intensities of lights. The location of the respective YqjM band is indicated with a red box and arrow- this location corresponds to a molecular weight of approximately 38.7 kDa (with an N-terminal His-Tag). LI1: 40-60 $\mu\text{E m}^{-2} \text{s}^{-1}$, LI2 and LI3: 150 $\mu\text{E m}^{-2} \text{s}^{-1}$.

Figure S2

Biotransformations using different substrate concentrations

Biotransformations were carried out with different substrate concentrations to investigate the dependency of enzymatic performance on the corresponding starting substrate concentrations.

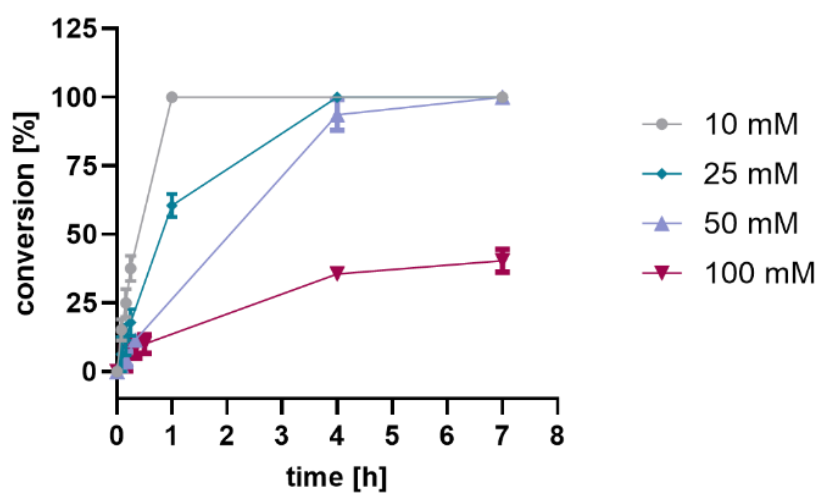


Figure S2 Whole cell biotransformations using Syn::*P_{cpc}-YqjM* were performed with different starting substrate concentrations. The graph depicts the conversion levels from **1a** to **1b** over time.

Figure S3

Steady state kinetics for YqjM

In order to determine K_M and v_{max} for the conversion of **1a**, steady state experiments were performed by following the oxidation of NADPH at 340 nm in a spectrophotometer using different concentrations of 2-methylmaleimide. The experiment was performed at 25 °C in 50 mM Tris-HCl, pH 7.5 containing 100 μM of NADPH and 100 nM final concentration of YqjM. Stock solutions of **1a** were prepared in the assay buffer and kinetic measurements were performed with final substrate concentrations of 25 – 5000 μM **1a**.

From the decrease of absorption and the extinction coefficient of NADPH, k_{obs} was calculated. Division of k_{obs} by the enzyme concentration results in k_{cat} values in the same magnitude of the reductive rate k_{red} which describes the reduction of flavin with NADPH. As this is the rate limiting step of the reaction, K_M and v_{max} for the conversion of **1a** could not be determined in the steady state kinetic experiments.

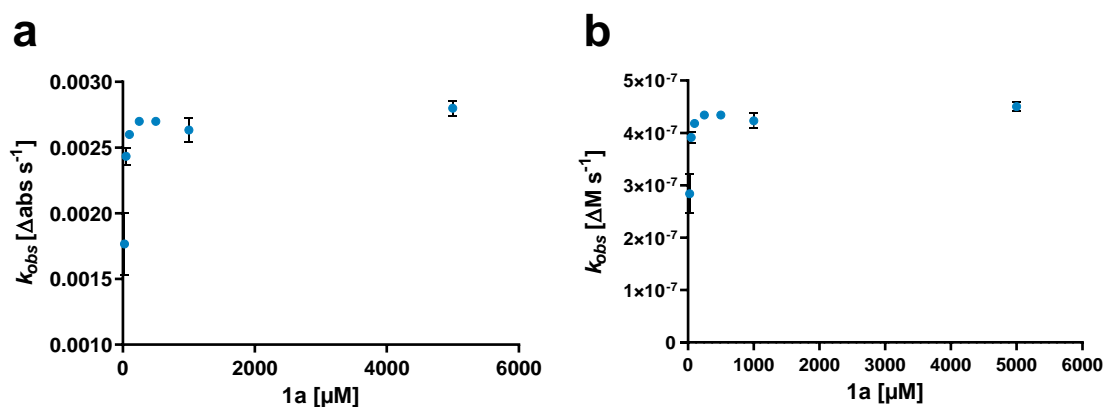


Figure S3 Steady state kinetic measurements for the reduction of **1a** with different substrate concentrations. **[a]** reflects the kinetics in terms of absorbance while **[b]** shows this in terms of changes in concentration.

Figure S4

P700 in the presence or absence of **1a**

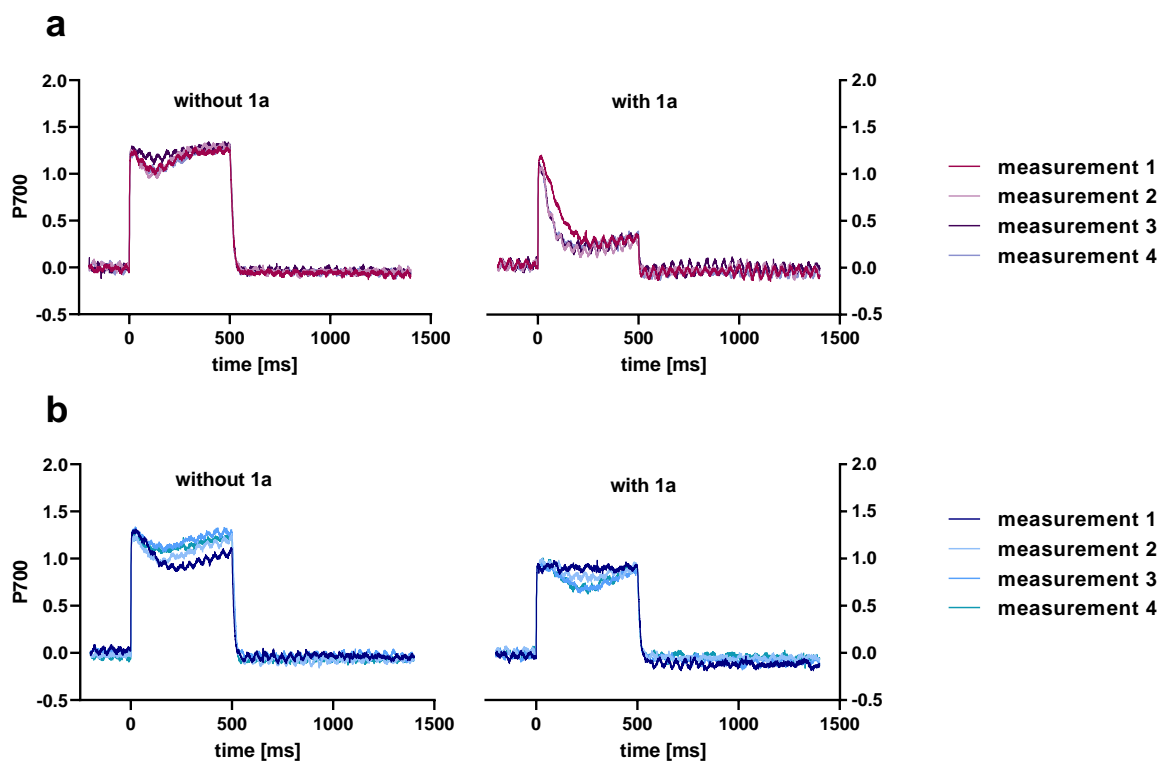


Figure S4 Measurements of P700 in **[a]** Syn WT and **[b]** its genetically modified counterpart that harbours the $P_{cpc}YqjM$ expression cassette ($Syn::P_{cpc}YqjM$) in the absence or presence of 50 mM of **1a**. Traces indicate the redox kinetics of P700 in the first, second, third and fourth saturating pulse ($500\mu s$, $5000\mu E m^{-2} s^{-1}$) under actinic red light ($50\mu E m^{-2} s^{-1}$). The figure denotes that in the absence of YqjM expression (panel **[a]**), **1a** causes a blockage in P700 oxidation which is rescued by the expression of YqjM (panel **[b]**). The kinetics are representatives of 2 biological replicates.

Figure S5

Viability assay with *Syn::P_{psbA2}YqjM*

2-MS was not toxic in concentrations up to 100 mM. However, the substrate **1a** decreased viability of cells tremendously. Wildtype cells died within 30 minutes when exposed to concentrations over 25 mM. In contrast, the recombinant strains could handle concentrations of 25 mM for 4 h. Decreased growth was observed for recombinant strains exposed to concentrations above 50 mM of **1a**. This means, cells required two weeks instead of one to grow back. A schematic representation of the growth behavior for wild type and *Syn::P_{cpc}YqjM* cells is given in (Figure 5c-d). The original plates are shown below.

Images were captured by the author H.C. Büchenschütz

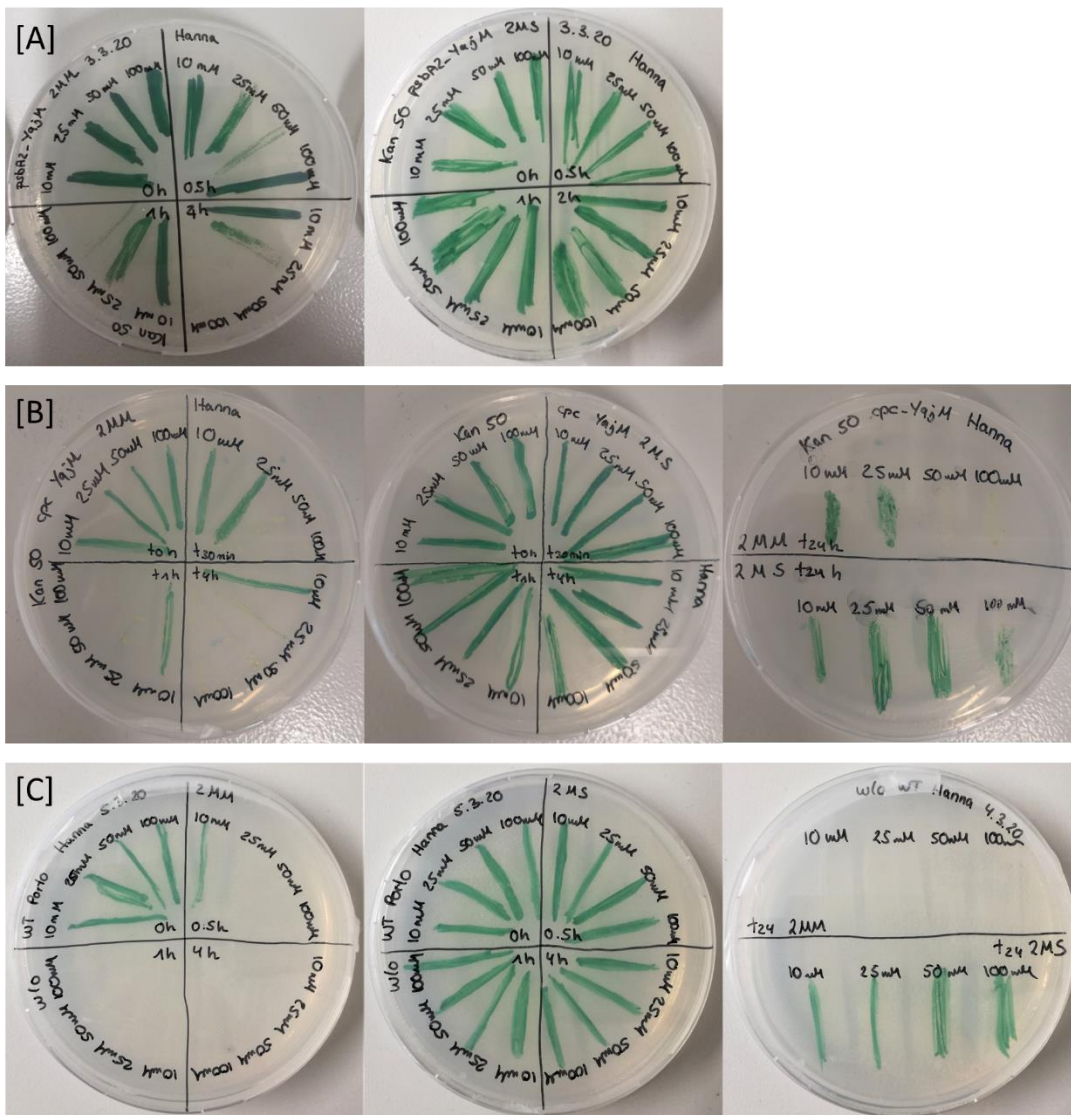


Figure S5 Viability assay with **[A]** *Syn::P_{psbA2}YqjM*, **[B]** *Syn::P_{cpc}YqjM* and **[C]** *Syn* WT in the presence of different concentrations of **1a** and **1b** over a time period of 4 – 24 h.

Figures S6, S7, S8

$\Delta Flv1::P_{cpc} YqjM$ biotransformations

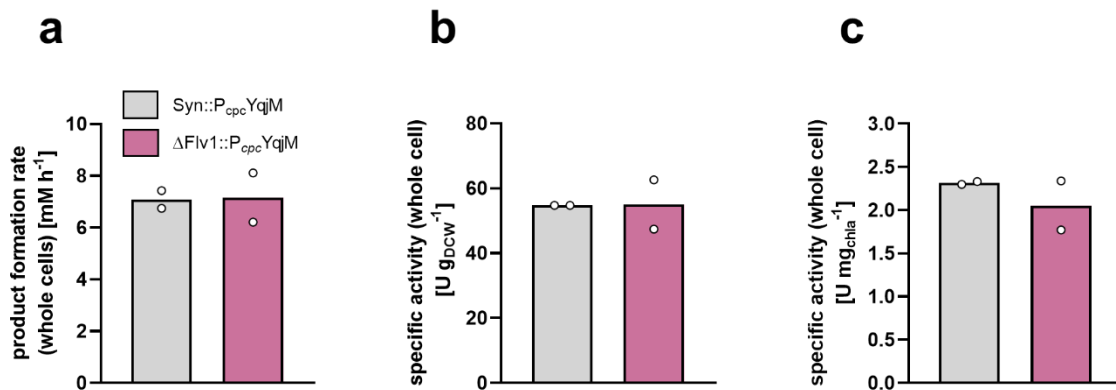


Figure S6 Product formation rate **[a]** and specific activity normalized to dry cell weight **[b]** and chl a content **[c]** for both Syn::P_{cpc}YqjM and $\Delta Flv1::P_{cpc} YqjM$. Cultures used to conduct the biotransformations were cultivated under blue-red plant growth lamps set to an average light intensity of 60 $\mu E m^{-2} s^{-1}$. At these conditions, no discernible differences were noted between the strains. Data used to create the panels is derived from biological replicates ($N=2$).

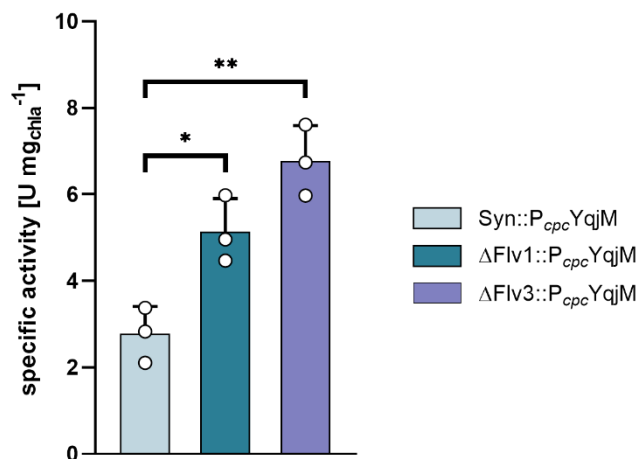


Figure S7 Chlorophyll a content normalized specific activity (main data shown in Figure 6). Values included stem from biological replicates ($N=3$). Statistical differences between Syn::P_{cpc}YqjM and the respective Flv deletion mutant is reported in the form of P values and was determined using Welch's t -test. ($*P < 0.05$, $**P < 0.01$)

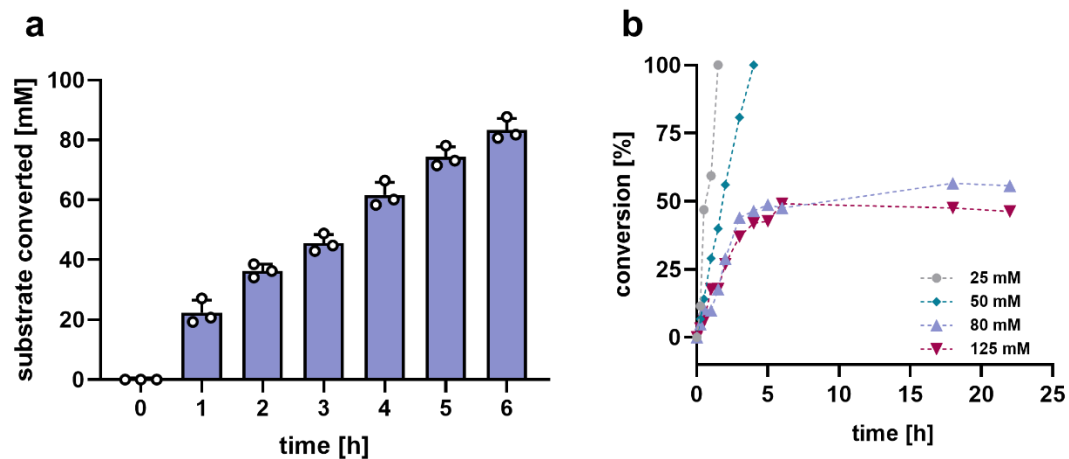


Figure S8 [a] Amount of **1a** converted by $\Delta Fiv1::P_{cpc}YqjM$ cells ($2.4 \text{ g}_{DCW} \text{ L}^{-1}$, $OD_{750} \sim 10$) using a substrate feeding approach. Initial substrate concentration introduced was 45.5 mM and a subsequent feeding of 16.14 mM, 14.88 mM and 12.1 mM was done at 3, 4 and 5 hours, respectively. With this approach, 100% of the substrate introduced was converted to the corresponding product (2-MS) in four hours and 94.04% was converted in 6 hours. Data plotted is derived from three biotransformations that stem from one harvested culture. **[b]** shows conversion of different **1a** concentration to the product 2-MS by $\Delta Fiv1::P_{cpc}YqjM$ cells ($2.4 \text{ g}_{DCW} \text{ L}^{-1}$, $OD_{750} \sim 10$)- in this experiment, the substrate was introduced fully from the beginning and no substrate feeding was utilized.

Figure S9

determination of light spectra

Plant growth lamps (CellDEG, Berlin, Germany) with red and blue LEDs were used for cultivation under different light intensities. These lamps have two adjustable switches, one for each LED color- in all cases, both switches were set to the same level. A spectrum for each LED color independently and both, operated concomitantly, was recorded using a diode array UV-Vis spectrometer (TIDAS UV-Vis spectrometer, J&M, Germany). These measurements were kindly performed by Dr. Dmytro Neshchadin from the Institute of Physical and Technical Chemistry (University of Technology, Graz). All three spectra are shown below.

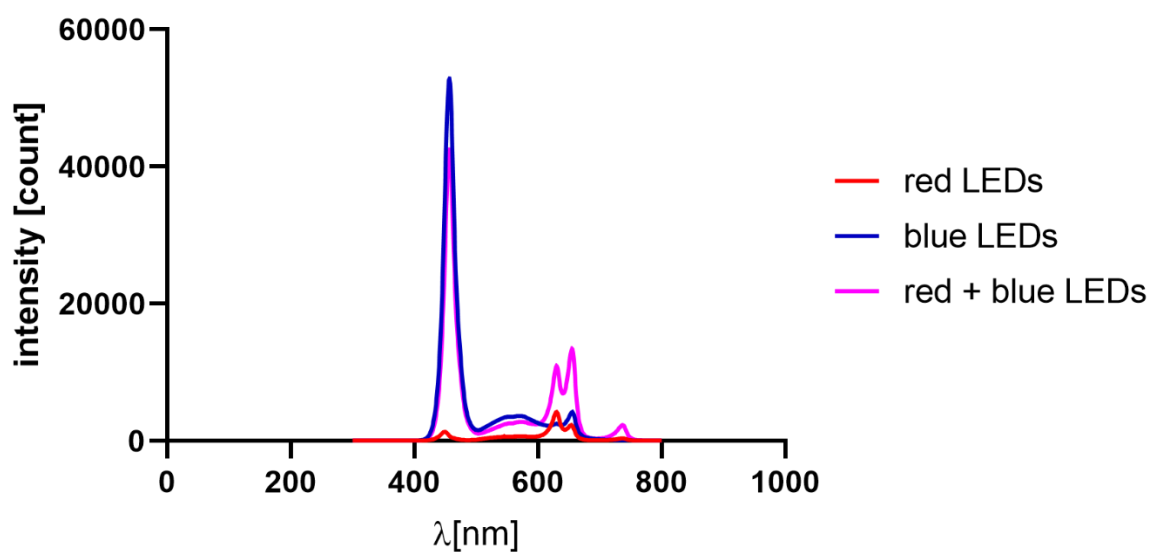


Figure S9 Spectra of the red-blue lamps used for cultivation under different light intensities. A spectrum for the individual red and blue LEDs as well as a spectrum of both LEDs on was recorded. The joined spectrum reflects the cultivation intensity under $150 \mu\text{E m}^{-2} \text{s}^{-1}$.

Figures S10 and S11

set up of high light cultivations and measurements

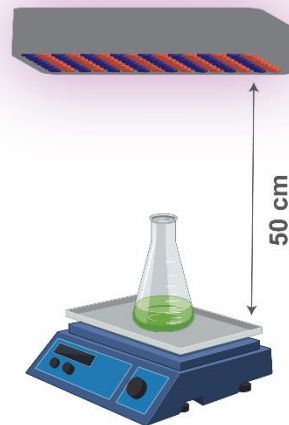


Figure S10 A graphical depiction of the set up used to culture *Synechocystis* cells with high blue-red light. The LED panel is suspended from roof with a distance of 50 cm between it and the rotary shaker. The rotary shaker has a maximum capacity of six 300 mL Erlenmeyer flasks. Image was created using BioRender and Illustrator CC.

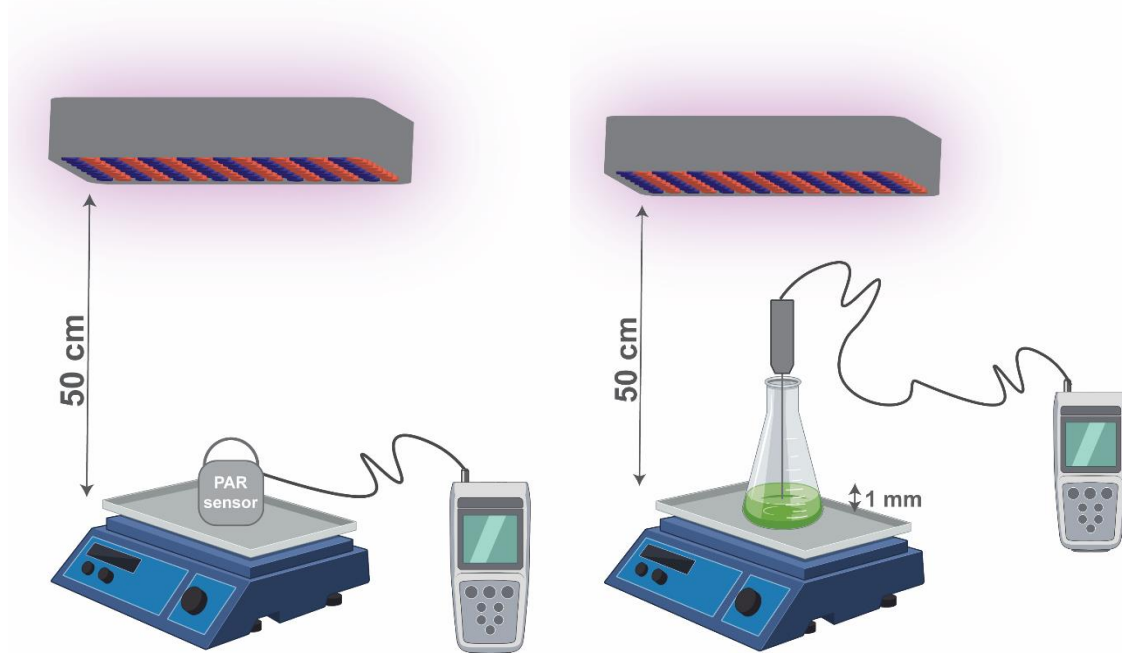


Figure S11 A graphical depiction of the set up used to measure light intensity in high blue-red light conditions. **Left** depicts measurement protocol with an externally attached PAR sensor. **Right** depicts measurement with the submersible quantum sphere sensor at a depth of ~1mm. These measurements were conducted with the shaker on or off and lasted a total of 15 seconds. The LED panel is suspended from the roof with a distance of 50 cm maintained between it and the rotary shaker. Image was created using BioRender and Illustrator CC. Values measured which were relevant to this work can be found in **Table S3** of this document.

Figure S12

The correlation between chlorophyll and optical density (OD_{750})

The amount of chlorophyll in correlation to OD_{750} for each strain was determined as described⁴ from samples originating from at least three independent cultivations under standard conditions. Cell culture (100 μ L) with a known OD_{750} was pelleted, resuspended in dH_2O (100 μ L) and filled with methanol (900 μ L). Samples were mixed and incubated in darkness (10 min). The absorption at 665 nm was measured and the amount of chlorophyll was determined using the extinction coefficient $\epsilon = 78.74 \text{ L g}^{-1} \text{ cm}^{-1}$. The corresponding graphs for the strains in this work can be found in **Figure S12**. A figure showing the correlation of optical density (measured at 750 nm) to cell dry weight can be found in **Figure S13**.

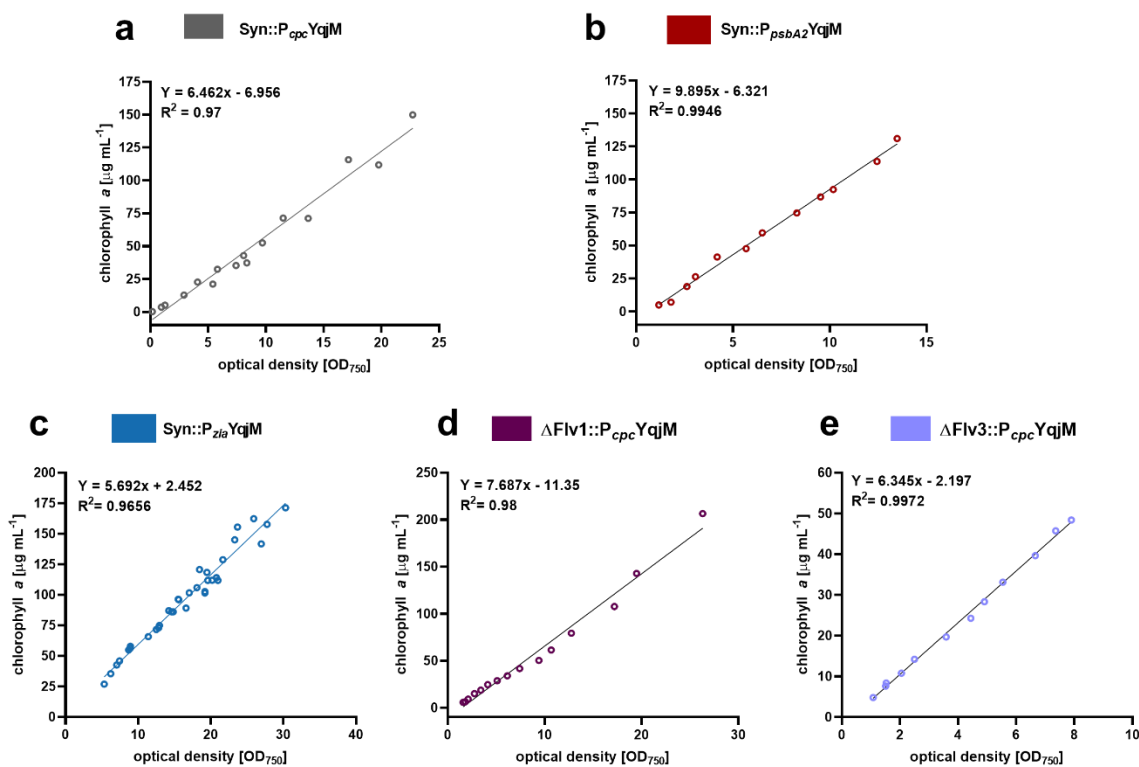


Figure S12 Correlation of optical density [OD_{750}] with the content of chlorophyll *a* for **[a]** $Syn::P_{cpc}YqjM$, **[b]** $Syn::P_{psbA2}YqjM$, **[c]** $Syn::P_{zia}YqjM$, **[d]** $\Delta Flv1::P_{cpc}YqjM$ and **[e]** $\Delta Flv3::P_{cpc}YqjM$. Corresponding line equations and R^2 values were calculated by fitting data points using a simple linear regression model and was not fitted through zero.

Figure S13

The correlation between optical density (OD_{750}) and cell dry weight

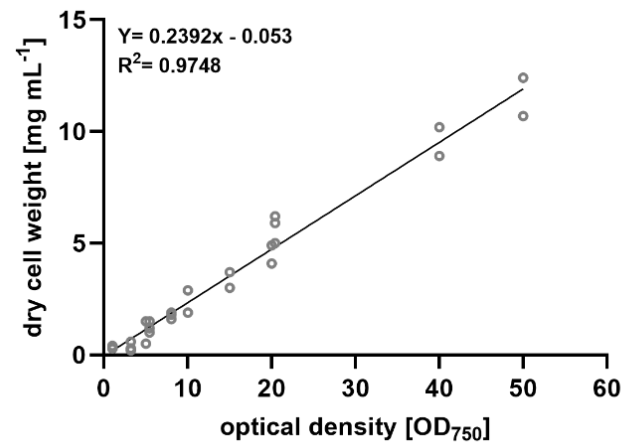


Figure S13 Correlation of optical density [OD₇₅₀] with dry cell weight of *Synechocystis* sp. PCC 6803. The corresponding line equation and R^2 value was determined by fitting data points using a simple linear regression model and was not fitted through zero.

Figure S14 and S15
Control reactions

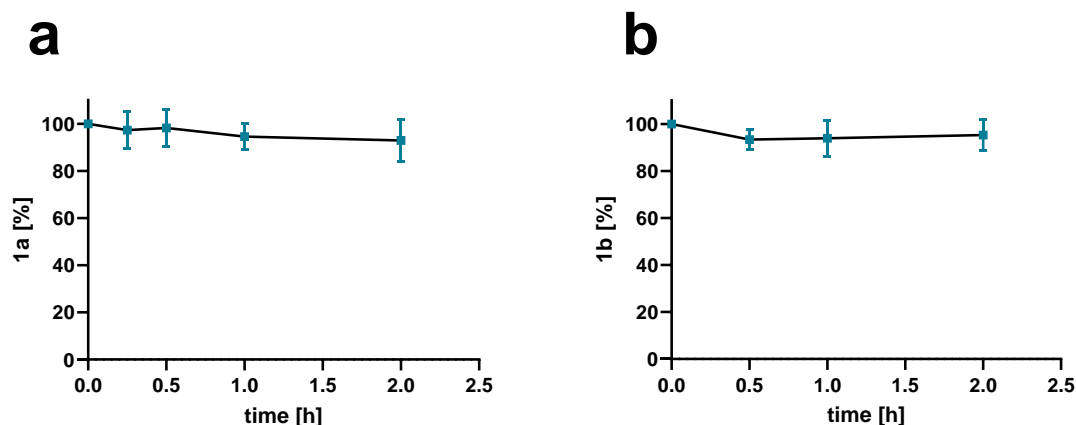


Figure S14 Controls were performed by the addition of [a] **1a** and [b] **1b** to ensure their stability over time. The, relatively, unchanged concentrations over time (expressed in terms of percentage detected compared to the starting concentration) confirm the stability of both the substrate and product over the time periods relevant for biotransformations. Data is derived from biological replicates ($N=3$) \pm S.D.

Various control reactions were carried out in darkness to determine how much of the resultant conversion may possibly be attributed to light and was carried out for all conditions discussed in this work. Additionally, controls using Syn WT, Δ Flv1 and Δ Flv3 are reported.

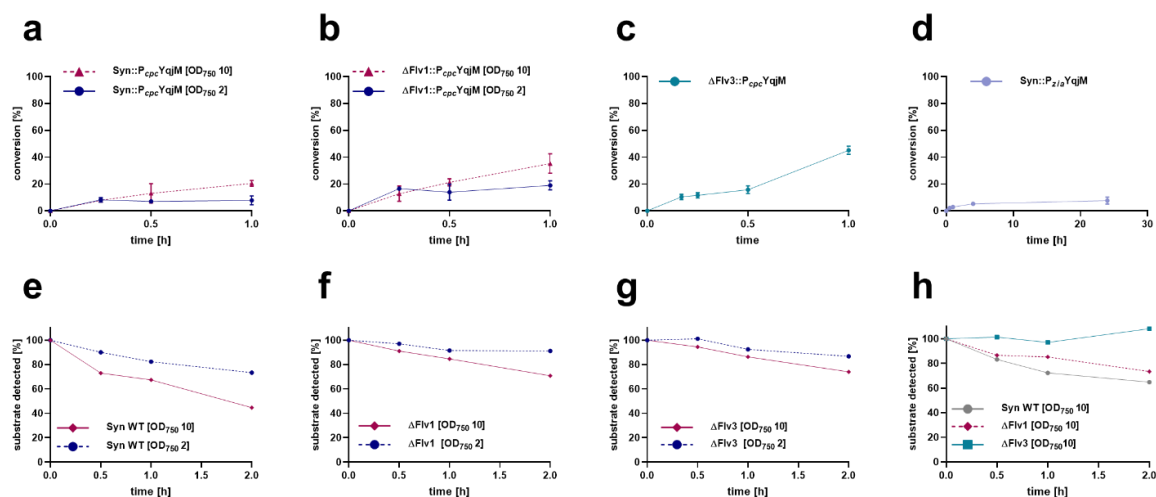


Figure S15 Various control reactions were carried out using the strains reported in this work. [a] and [b] show conversions of control biotransformations, in darkness, using 10 mM of **1a** in cultures with optical densities (OD₇₅₀) of 10 and 2 of Syn::P_{cpc}YqjM and Δ Flv1::P_{cpc}YqjM, respectively. [c] and [d] depict control biotransformations of 10 mM **1a** in the darkness using, respectively, Δ Flv3::P_{cpc}YqjM and Syn::P_{Zia}YqjM cultures at an OD₇₅₀ of 10. Panels [e – g] show substrate found in reactions using strains that did not express YqjM (Syn WT, Δ Flv1 and Δ Flv3, respectively) at OD₇₅₀ of 10 and 2. These controls were conducted in light conditions (150 μ E m⁻² s⁻¹). Panel [h] shows substrate detected in reactions using Syn WT, Δ Flv1 and Δ Flv3 at an OD₇₅₀ of 10 and were conducted in the dark. Data used to plot panels [a-d] stems from biological replicates ($N=3$).

Figure S16 and S17

Example graphs of *in vitro* determination of relative YqjM values and determination of extinction coefficients.

Examples for typical graphs from the raw data generated by *in vitro* cofactor (NADPH or NADH) assays to determine relative YqjM values is depicted in **Figure S16**. The decrease of the absorption at 340 nm differs between strains that express YqjM under the control of different promoters, P_{zia} , P_{psbA2} or P_{cpc} . This indicates that the crude cell extract has different concentrations of YqjM, thus signaling differences in expression capacity based on the promoter occupied.

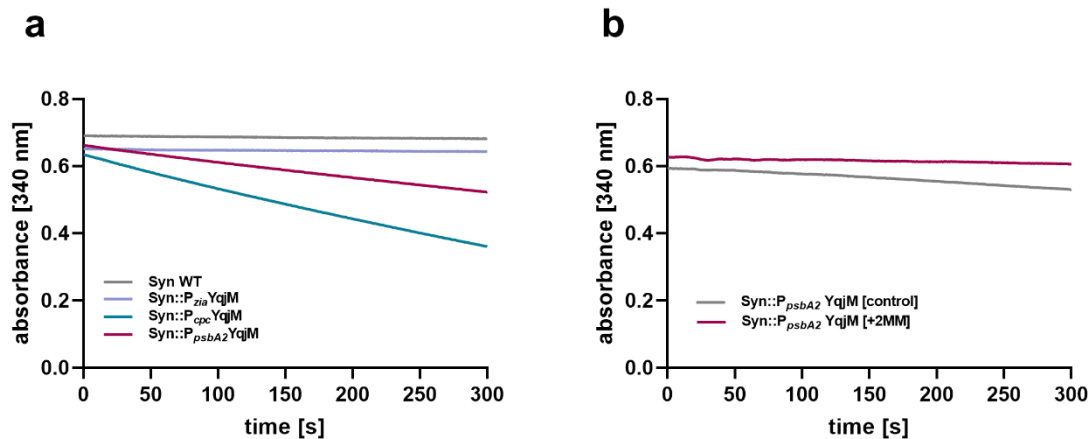


Figure S16 Exemplary image depicting typical drops in **[a]** NADPH absorbance over time in multiple strains in the presence of 1 mM of **1a**. **[b]** depicts example results from the same *in vitro* test, but with NADH being employed as the cofactor. As clearly visible, the consumption of NADH is almost negligible compared to NADPH for the same strain Syn::P_{psbA2} YqjM.

As known from literature,^{5,6} YqjM can accept both NADPH and NADH. Our study revealed, that it has a 10-time higher affinity toward NADPH. We showed this by a detailed investigation of the kinetics and it is also reflected by the *in vitro* NADPH-assay.

The extinction coefficient $\epsilon_{\text{NADPH}} = 0.0045 \text{ L } \mu\text{mol}^{-1} \text{ cm}^{-1}$ and $\epsilon_{\text{NADH}} = 0.0045 \text{ L } \mu\text{mol}^{-1} \text{ cm}^{-1}$ were determined according to Lambert-Beer law (Equation 1). Therefore, absorption at 340 nm of different NAD(P)H concentrations was measured and plotted to obtain the slope (**Figure S18**). Commercial cuvettes with $d = 1 \text{ cm}$ were used. $A_{340 \text{ nm}} = \epsilon * d * c$

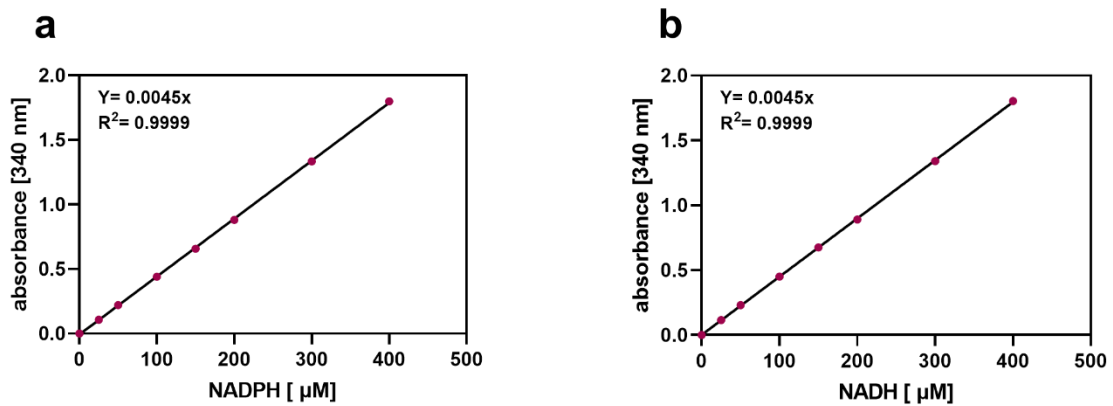


Figure S17 Correlation of absorption at 340 nm with the concentration of **[a]** NADPH and **[b]** NADH. According to the Lambert Beer law, the extinction coefficient ϵ corresponds to the slope.

Figure S18 and S19

GC-FID calibrations curves and example chromatogram

Samples were analysed by gas chromatography (GC) using SHIMADZU GC-2010 Plus instrument equipped with a flame-ionization detector (FID) and a Zebron ZB-5 column. The quantification of the compounds was set up using 1-decanol (2 mM) as an internal standard. The calibration curve for **1a** and **1b** include data from two independent technical replicates (Figure S18). An example chromatogram is shown in Figure S19.

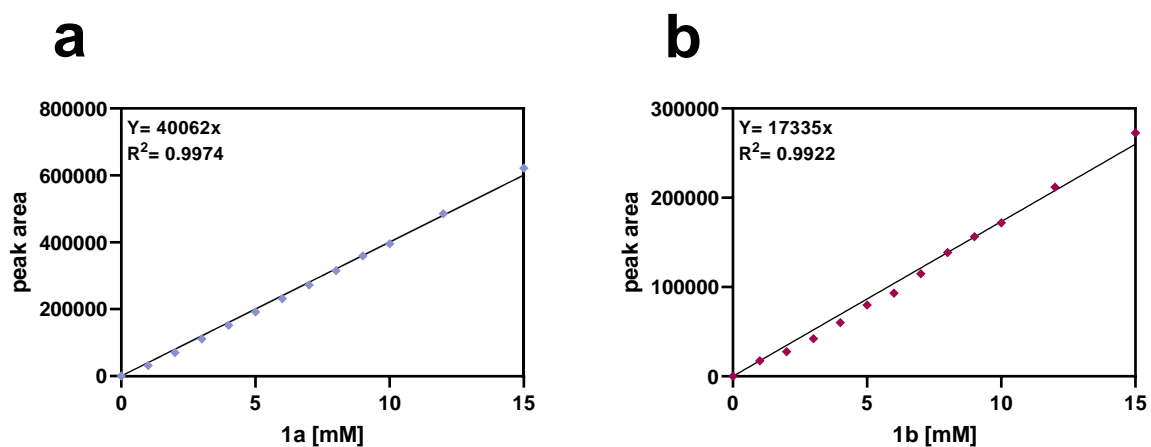


Figure S18 Standard curves generated for chromatographic analysis of [a] **1a** and [b] **1b**. Data from two independent technical replicates are included and the corresponding line equations and R^2 values were generated by a simple linear regression and was forced through zero.

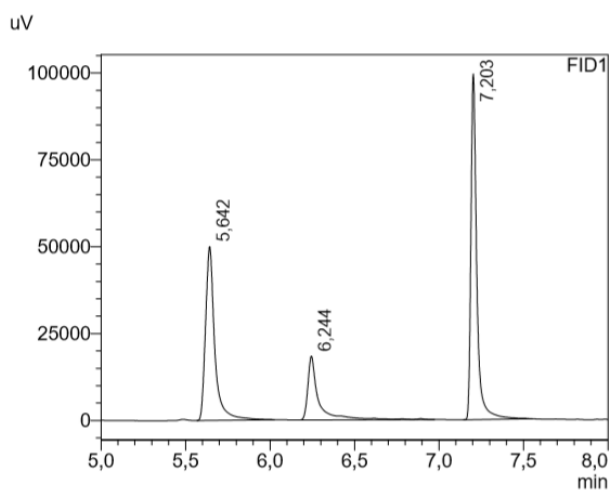


Figure S19 Example GC-Chromatogram showing **1a** (ret. time 5.6 min) and **1b** (ret. time 6.2 min). 1-decanol (ret. time 7.2 min) was used as an internal standard.

References

- (1) Königer, K.; Gómez Baraibar, Á.; Mügge, C.; Paul, C. E.; Hollmann, F.; Nowaczyk, M. M.; Kourist, R. Recombinant Cyanobacteria for the Asymmetric Reduction of C=C Bonds Fueled by the Biocatalytic Oxidation of Water. *Angew. Chem. Int. Ed.* **2016**, *55* (18), 5582–5585.
- (2) Stanier, R. Y.; Kunisawa, R.; Mandel, M.; Cohen-Bazire, G. Purification and Properties of Unicellular Blue-Green Algae (Order Chroococcales). *Bacteriol. Rev.* **1971**, *35* (2), 171–205.
- (3) Mustila, H.; Paananen, P.; Battchikova, N.; Santana-Sánchez, A.; Muth-Pawlak, D.; Hagemann, M.; Aro, E.-M.; Allahverdiyeva, Y. The Flavodiiron Protein Flv3 Functions as a Homo-Oligomer During Stress Acclimation and Is Distinct from the Flv1/Flv3 Hetero-Oligomer Specific to the O₂ Photoreduction Pathway. *Plant Cell Physiol.* **2016**, *57* (7), 1468-1483.
- (4) Schuurmans, R. M.; van Alphen, P.; Schuurmans, J. M.; Matthijs, H. C. P.; Hellingwerf, K. J. Comparison of the Photosynthetic Yield of Cyanobacteria and Green Algae: Different Methods Give Different Answers. *PLOS ONE* **2015**, *10* (9), e0139061.
- (5) Fitzpatrick, T. B.; Amrhein, N.; Macheroux, P. Characterization of YqjM, an Old Yellow Enzyme Homolog from *Bacillus Subtilis* Involved in the Oxidative Stress Response. *J. Biol. Chem.* **2003**, *278* (22), 19891–19897.
- (6) Pesic, M.; Fernández-Fueyo, E.; Hollmann, F. Characterization of the Old Yellow Enzyme Homolog from *Bacillus Subtilis* (YqjM). *ChemistrySelect* **2017**, *2* (13), 3866–3871.